Relationship of solubility parameter (x), powder properties and phase formation in the $Nd_{1+x}Ba_{2-x}Cu_3O_{6.5+x/2+\delta}$ system

P. Yossefov [a], G.E. Shter [a], G.M. Reisner [a], A. Friedman [b], Y. Yeshurun [b], G.S. Grader [a]

[a] *Chemical Engineering Department, Crown Center for Superconductivity, Technion, Haifa 32000, Israel*
[b] *Center for Superconductivity, Department of Physics, Bar-Ilan University, Ramat-Gan 52900, Israel*

Abstract

The relationship between the solubility parameter, x, in the solid solutions $Nd_{1+x}Ba_{2-x}Cu_3O_{6.5+x/2+\delta}$ (Nd123SS) and XRD patterns, powder surface area (SA), particle size, morphology and melting points was investigated. An efficient way to determine the value of x and residual $BaCuO_2$ content during Nd123SS powder synthesis is presented. The method is based on calculation of the orthorhombic splitting (OS) factor from the unit cell parameters obtained from XRD data. The final phase in the Nd123SS system is formed through a diffusion controlled reaction between $BaCuO_2$ and Nd123SS and a kinetic model is developed to describe the formation of the Nd123 ($x = 0$) superconducting powder. Finally, high values of T_c (measured by DC magnetization) were found in the powders. The highest T_c of 98.7 K was measured for the $x = 0$ case. This value is the highest ever reported for the Nd–Ba–Cu–O system. The T_c was found to be insensitive to the value of x, ranging between 98.7 and 94 K for x between 0 and 0.25, respectively. This data is in contrast to published results on samples synthesized at higher temperatures, where T_c fell to 40 K at $x = 0.25$.

Keywords: Superconductor; $Nd_{1+x}Ba_{2-x}Cu_3O_{6.5+x/2+\delta}$; Solid solution; Phase formation

1. Introduction

Recently, it has been shown that substituting Nd for Y in the $YBa_2Cu_3O_{7-\delta}$ (Y123) melt textured superconductors improves the critical current (j_c) under large magnetic fields [1–5]. This makes Nd123 material attractive and vital for high-field applications. Rare earth elements (RE) readily substitute for Y to give RE123 superconductors. Since the ionic radii of the light RE elements (i.e. Nd, La and Sm [6–12]) approach that of the Ba, a solid solution can be formed with a large degree of substitution of the RE on the Ba site. For example, a neutron diffraction study of $Nd_{1.2}Ba_{1.8}Cu_3O_{6.6+\delta}$ has revealed that 0.2 neodymium ions per formula unit occupy the Ba-site in addition to the Nd-site [13]. The ionic difference between Nd^{+3} (0.129 nm) and Ba^{+2} (0.161 nm) is smaller than that between the radii of Y^{+3} (0.102 nm) and Ba^{+2}. Thus, unlike Y123, the Nd123 system exhibits a solid solution of the form $Nd_{1+x}Ba_{2-x}Cu_3O_{6.5+x/2+\delta}$ (Nd123SS). The solubility range is reported to be $0.04 \le x \le 0.6$ [7,14,15]. At this paper, x is called the solubility parameter.

Some of the important observations, concerning the Nd123SS compounds are: (i) in the fully oxy-

genated state, an orthorhombic to tetragonal (OT) phase transformation occurs when x is increased from 0.15 to about 0.25 [6,8,11,12]; (ii) due to the higher valence state of Nd ions, the oxygen content in the compound, increases with the rise of x [6]; (iii) drastic decrease of the critical temperature at $x > 0.1$ was observed [10–12,14–16]. However, no systematic work on the dynamic changes and the absolute value of x in the NdBaCuO system during synthesis has been published to the best of our knowledge. In addition, the melting points and morphological changes of the Nd123SS as a function of x have not been determined. The solid state reactions leading to the Nd123 phase have not been reported either.

In this work, it is shown that during calcination of powders in the NdBaCuO system, a solid solution (Nd123SS) and $BaCuO_2$ are first formed. In the following stage, these components react until all the $BaCuO_2$ is consumed forming the final solid solution composition. Knowledge of the $BaCuO_2$ content in the powder is important for monitoring the reaction progress, however small peaks in X-ray diffractograms cannot indicate that its amount is negligible [17].

The main objectives of the present work are: (i) to investigate the effect of x on the unit cell parameters, the orthorhombicity, the melting point, the surface area and the morphology of Nd123SS powders; (ii) to improve the evaluation of x in different Nd123SS powders, using X-ray diffraction (XRD) data; (iii) to find the relationship between x and the amount of the secondary phase $BaCuO_2$ formed during Nd123 synthesis; (iv) to study, for the first time, the Nd123 phase formation using x as a kinetic parameter under different calcination conditions; and finally (v) to determine the dependence of the critical temperature on x for the Nd123SS powders calcinated at low temperature.

2. Experimental procedure

Solid solutions of $Nd_{1+x}Ba_{2-x}Cu_3O_{6.5+x/2+\delta}$ powders having compositions of $x = 0.0, 0.05, 0.10, 0.15, 0.20, 0.225$ and 0.25 were prepared by the oxalate coprecipitation route. The synthesis proce-

dure includes the following stages; (i) an oxalate coprecipitation [18,19] of the metal acetates of Neodymium, Barium and Copper with the desired stoichiometry; (ii) precalcination of the coprecipitated powders at 700°C for 3 hours in air in order to oxidize the oxalates, giving a mix of Nd_2CuO_4, CuO and $BaCO_3$; (iii) vacuum preheating (10 Pa) of the powders at 770°C for 20 hours in order to ease the $BaCO_3$ decomposition; (iv) calcination under an atmosphere of 0.1 or 1% O_2 in N_2 at the temperature range 780–860°C for 2–20 hours, followed by annealing under pure O_2 at 450°C for 5 hours. Based on the literature [20] and the small particle size involved ($0.2 < 2$ μm), the annealing time is sufficient to saturate the oxygen content of the Nd123SS powders.

The XRD data were collected using a D5000 Siemens powder diffractometer employing Cu-Kα radiation. The 2-theta (2θ) range (6° to 140°) was scanned in steps of 0.02° with a counting time of 8 sec/step. The power conditions were 40 kV at 40 mA. Lattice parameters were determined using a least squares fitting program. The surface area of the powders was measured by N_2 adsorption at 77 K (Micromeritics Flowsorb II 2300). Simultaneous DTA and TGA were performed on the powders at a heating rate of 5°C/min in air using the Setaram TG-92 analyser. Scanning electron microscopy (SEM) was carried out using a Jeol 5400 instrument. DC magnetization measurements were performed on a quantum Design SQUID magnetometer. In all these measurements the sample was cooled to 10 K in zero field; the field of 50 G was then applied and the temperature dependence of the magnetization was measured between 10 and 110 K.

3. Results and discussion

The X-ray powder diffraction patterns of the different solid solutions of $Nd_{1+x}Ba_{2-x}Cu_3O_{6.5+x/2+\delta}$ with $x = 0, 0.05, 0.10, 0.15, 0.20$ and 0.25 are shown in Fig. 1. No secondary phases were detected by XRD, implying that the volume of the detected phase is at least 98%. The samples were also checked by DTA/TGA in the range 25–1200°C and only one peak was observed at the melting points, consistent

with the samples being of single phase. The main reflections, demonstrating the changes in the Nd123SS cell parameters are: (013) and (103) at $2\theta = 32\text{–}32.8°$, (020) and (200) at $2\theta = 46\text{–}47.3°$, and (123) and (213) at $2\theta = 57.5\text{–}58.5°$. The splittings of these reflections indicate changes in the orthorhombicity of the Nd123SS cell. Each pair of the above reflections is accompanied by additional overlapping reflections (110), (006) and (116), respectively. The data represented in Fig. 1a clearly demonstrates the decrease in the orthorhombic splitting (the separation of the reflections that distinguish between a and b) with increasing solubility parameter, x. Above $x = 0.225$ a doublet occurs due to the difference between the a and $c/3$ parameters (for

Fig. 2. Effect of x on (a) the unit cell parameters and (b) the orthorhombic splitting (OS) factor of Nd123SS powders.
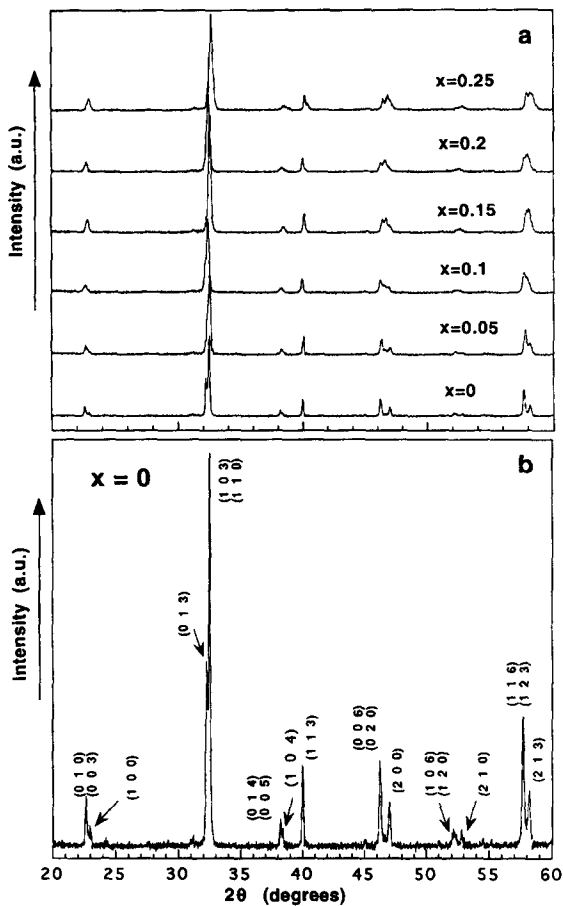

Fig. 1. (a) XRD patterns of Nd123SS powders for different x values and (b) the characteristic reflections of orthorhombic Nd123 ($x = 0$) characteristic reflections.
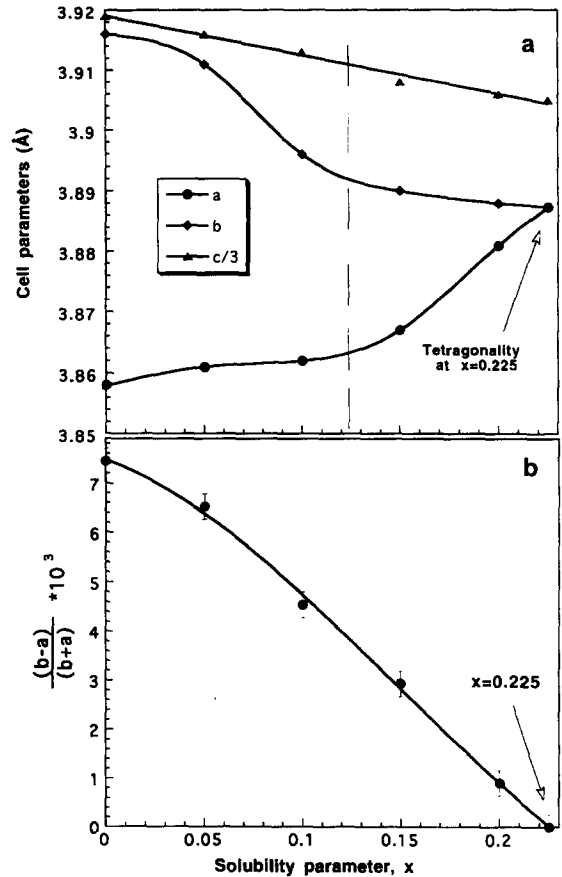
example, between (123) and (116), and between (200) and (006) reflections). Fig. 1b illustrates the XRD pattern of orthorhombic Nd123 ($x = 0$) with the mentioned overlapping reflections.

The effect of x on the unit cell parameters is demonstrated in Fig. 2a. These lattice parameter changes agree closely with previous reports [6,21,22]. Numerous studies (for example Refs. [20,23–28]) indicate that the oxygen in-diffusion is anisotropic and is much faster in the ab plane than in the c direction. Hence, changes in the c direction are not expected to be as drastic as in the ab directions. The data in Fig. 2a show that c decreases slowly and linearly, while a and b change more drastically. There are discrepancies concerning the oxygen content changes in the Nd123SS materials as a function of x. Fomichev et. al [29] found that for

$Nd_{1+x}Ba_{2-x}Cu_3O_{7-\delta'}$, δ' increases with x. If the formula is written as $Nd_{1+x}Ba_{2-x}Cu_3O_{6.5+x/2+\delta}$ (where $1/2 - \delta' = x/2 + \delta$), it can be seen from their results that δ is constant as x increases. In other words, the apparent increase in the oxygen content is merely due to the higher valence state of Nd relative to Ba. In our work, the annealing time is long enough to saturate the Nd123SS grains (diameter < 2.0 μm) with oxygen, and δ is therefore assumed to be constant.

The changes of a and b with x (Fig. 2a) can be separated into two stages: first a barely changes and b decreases rapidly until x approaches 0.13, and then a increases rapidly while b decreases slowly as x approaches 0.225. According to the $Nd_{1+x}Ba_{2-x}Cu_3O_{6.5+x/2+\delta}$ cell structure [30] and nomenclature [26], the oxygen sites O(5) and O(1) (in directions a and b, respectively) are located in the basal plane. In the calcination stage (840°C, 0.1% O_2), the cell structure of the solid solutions is in all cases tetragonal. Upon cooling to the annealing temperature, oxygen diffuses into the lattice. From Fig. 2a it is seen that in the $0.13 < x \le 0.225$ range, the O(1) site (along b) remains with the same occupancy while the O(5) site (along a) absorbs less oxygen as x decreases. In the $0 \le x \le 0.13$ range, the O(5) site is practically empty while the O(1) site absorbs an increasing amount of oxygen as x decreases. It should be noted that the overall oxygen content in the material ($6.5 + x/2 + \delta$) decreases as x decreases. The effect above is not of a kinetic origin since the samples are allowed to reach equilibrium at 450°C in flowing oxygen. This effect is clearly related to the higher oxidation state of the Nd relative to the Ba. However, an exact explanation should be based on cell structure simulation.

It is common to define the orthorhombic splitting (OS) in the unit cell by the expression:

$$OS = \frac{(b-a)}{(b+a)} 1000. \qquad (1)$$

Eq. (1) is widely used to describe changes in the orthorhombicity of the Y123 unit cell with oxygen content. Here it will be used to describe the orthorhombicity changes in the Nd123SS cell with changes in x. The effect of x on the OS is demonstrated in Fig. 2b. Increasing x increases the lattice

symmetry and reduces the OS. The OS disappears at $x \approx 0.225$ with transition to a tetragonal structure. Another good indication to the orthorhombicity of the Nd123SS unit cell is the separation (in degrees) of the previously mentioned reflections. The most sensitive reflections are the (020) and (200). The changing pattern of the (006), (020) and (200) reflections at various x values is represented in Fig. 3. Along with the decrease of the splitting of the (200) and (020) reflections with increasing x, the intensity of the reflections changes due to the separation of the peaks. For $x > 0.05$ the difference between b and $c/3$ increases (see Fig. 2a), the reflections separate and three different peaks appear.
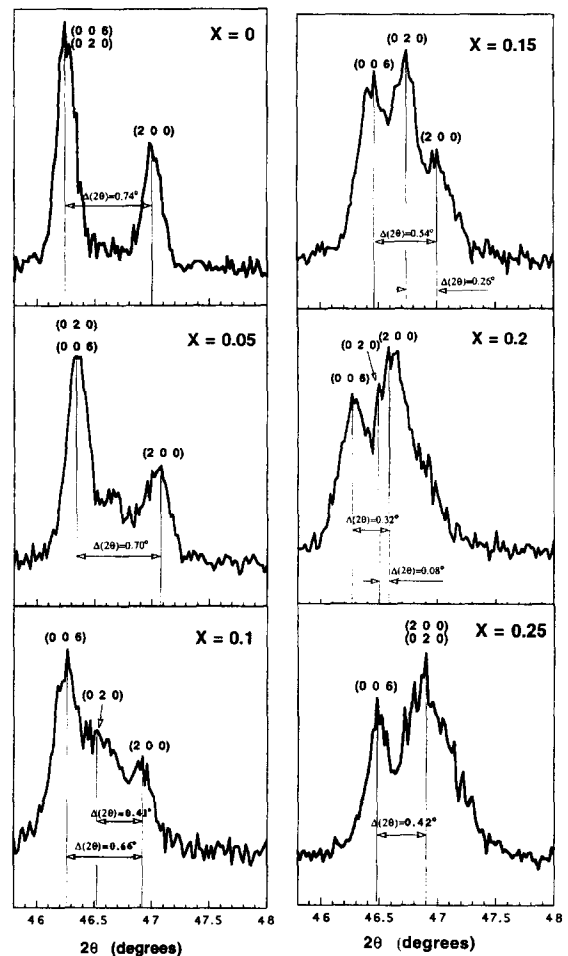

Fig. 3. Effect of x on the changing pattern of the (020) and (200) reflections.

The separation ($\Delta(2\theta)$) of the (020) and (200) reflections as a function of x is shown in Fig. 4a and 4b. The separation was calculated by: (1) direct measurement from the diffractogram (Fig. 4a), and (2) calculation using the Bragg law after evaluating the cell parameters by the least square program (Fig. 4b). The expression for the orthorhombic splitting width is given by:

$$\Delta(2\theta)_{(200)-(020)} = 2[\arcsin(\lambda/a) - \arcsin(\lambda/b)]. \quad (2)$$

At small x in Fig. 4a, the fit is poor due to the overlap between the (020) and the (006) reflections. The fit in Fig. 4b is better since the cell parameters can be accurately calculated. Fig. 4a and 4b provide, for the first time, a quick way to predict the value of x in the Nd123 system during its preparation.

SEM micrographs of Nd123SS powders (prepared at 840°C, 12hr, 0.1% O_2) illustrate the effect of x on the morphology of the powders. As shown in Fig. 5, the average particle size decreases with increasing x, from about 1–2.5 μm at $x = 0$ down to 0.2–0.5 μm at $x = 0.25$. The particles at $x \le 0.05$ are rounded and connected indicating that the powder started to sinter in the presence of a liquid phase. For $x > 0.05$, the grains are separated and their shape is in most cases rectangular. The quantity of the liquid phase (containing CuO and $BaCuO_2$) is less than 2% volume (the diffractometer limit) since it is not observed by XRD and therefore could not be identified.

The changes in the morphology of the powders are also reflected in the surface area (SA), as shown in Fig. 6. The SA of the different powders decreases as x decreases leading to a nearly ten-fold difference in the SA between $x = 0$ and $x = 0.25$. The data of this figure implies an exponential effect of x on the surface area. The effect of the calcination time on the surface area of the solid solutions is also illustrated in Fig. 6. In all cases the powders were single phased as demonstrated by XRD. It can be seen that the SA after 32 hours of calcination is only slightly lower than the 12 hour analog. As will be shown shortly, the Nd123 powder forms via a solid state reaction between $BaCuO_2$ and Nd123SS. As x decreases the particle growth is accelerated and the surface area is decreased. Once the reaction is completed (i.e. $x = 0$), the effect of extra calcination time on the surface area is relatively small. Hence we postulate that the

described solid state reaction at large x is diffusion limited. In addition, the excess Nd acts like a grain growth inhibitor and, thus at $x > 0.05$ the surface area is much higher than at lower x values.

Thermal analysis was carried out for the Nd123SS coprecipitated oxalate powders under air. Before the melting point, the powders were quenched and found to be single phased by XRD analysis. It has been found that the onset of melting (solidus points) depends on x. As demonstrated in Fig. 7, the melting points decrease monotonically from 1093°C at $x = 0$ to 1076°C at $x = 0.25$. The above characterization methods are convenient ways to evaluate x during Nd123SS powders preparation. However, the recommended way to evaluate x is to use the OS factor which is sensitive to the value of x and is easy to
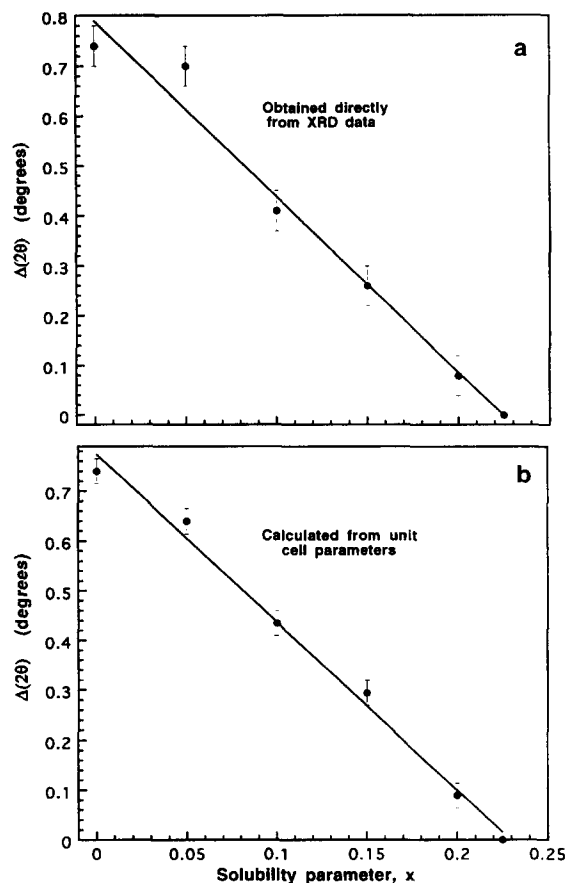

Fig. 4. The separation of the (020) and (200) reflections as a function of x obtained by (a) direct measurement from the diffractograms and (b) from the unit cell parameters.
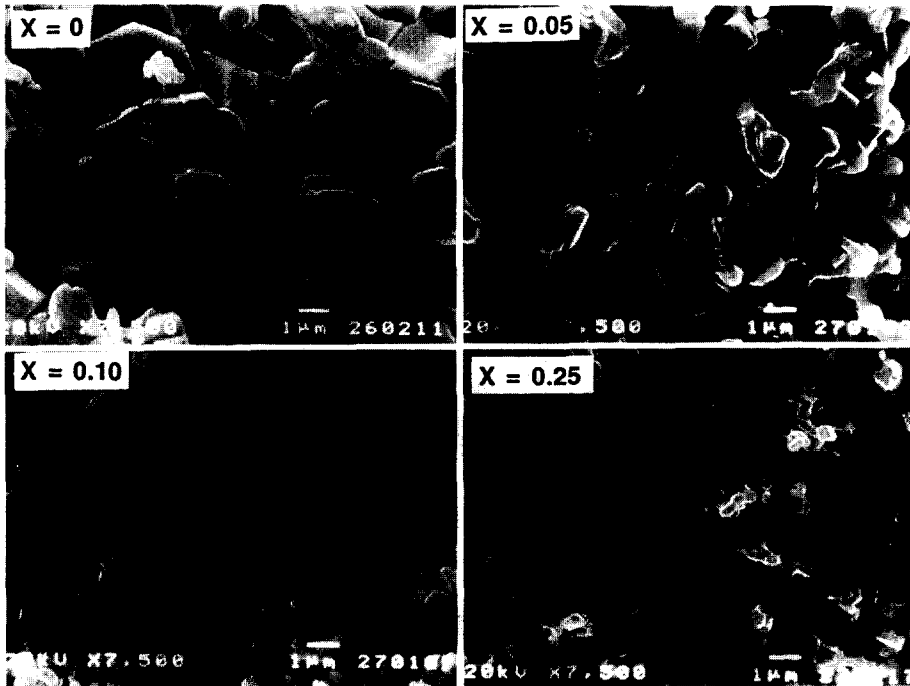
Fig. 5. SEM micrographs of Nd123SS powders at different values of x.

calculate once the cell parameters are found from XRD data.

The critical temperature of our samples does not depend on x in such a drastic way as in the previous works on the samples calcined at higher temperatures (Table 1). As seen in Fig. 8a the magnetic
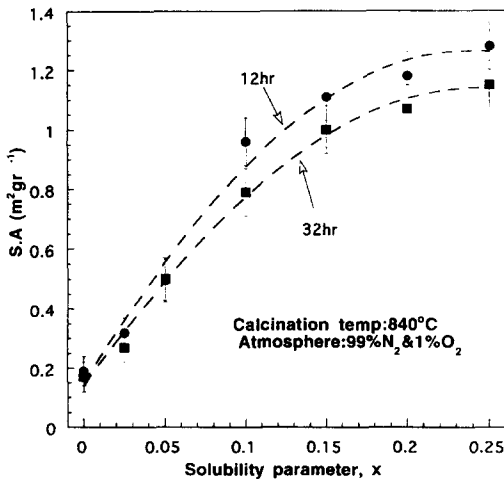
moments decrease monotonically with temperature for all x-values. In general the $M(T)$ curves show clearly a single superconducting phase and a well
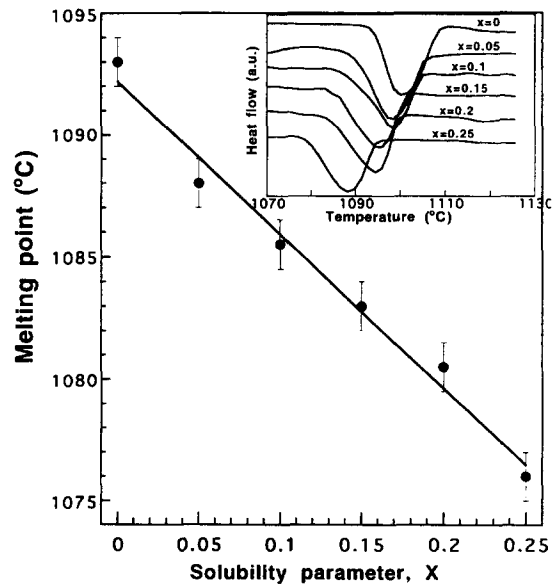

Fig. 6. Effect of x on the surface area of Nd123SS powders at different calcination times.

Fig. 7. Effect of x on the melting points of oxalate derived Nd123SS powders.

Table 1
Comparison of T_c of $Nd_{1+x}Ba_{2-x}Cu_3O_{6.5+x/2+\delta}$ powders obtained here and elsewhere, in the $0 \leq x \leq 0.25$ range

x	Our results	Kramer et al. [a] [15]	Takita et al. [a] [16]	Murakami et al. [1]
0	98.7	88	90	96.2
0.05	98.6	87		
0.1	98.3	80	80	
0.15	94	60		
0.2	96.1	43	50	
0.25	97.4	40		

[a] The values of T_c were taken from figures.

pronounced transition temperature for all x (Fig. 8b). The absolute value of the magnetic moment decrease substantially with increasing x (see Fig. 8a). This can be associated with either decrease in Meisner fraction or with the observed decrease of the particle sizes with x. We believe that these remark-

Fig. 9. XRD patterns of Nd123 powders calcined at different temperatures.

able results are due to the low temperature synthesis, where secondary phases due to peritectic reactions are avoided. The earlier work [15,16] (see Table 1) were carried at higher temperatures where such reactions are present.

The second part of this paper is aimed at using x as a kinetic parameter in the formation of $NdBa_2Cu_3O_{6.5+\delta}$ (Nd123) superconducting powder. For this purpose, calcination was performed in temperature range 780–840°C under an atmosphere of 99% N_2 and 1% O_2 for 2–32 hours. The initial SA and particle size were 5–6 m^2/gr and 0.1–0.2 μm, respectively. These parameters were kept constant in all the starting powders. As stated earlier, the synthesis of the Nd123 powder undergoes a solid state reaction described in general by:

$$\frac{3x}{1+x}BaCuO_2 + \frac{1}{1+x}Nd_{1+x}Ba_{2-x}Cu_3O_{6.5+x/2+\delta}$$
$$\rightarrow NdBa_2Cu_3O_{6.5+\delta}. \qquad (3)$$
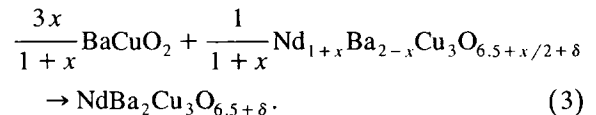
The experimental indication for the occurrence of this reaction is given by the diffractograms presented in Fig. 9. In the state of uncompleted reaction (780°C, 6 hr), we observed a significant amount of $BaCuO_2$ along with weak orthorhombic splittings of the characteristic reflections (for instance (200) and (020)), indicating the existence of a solid solution. No other phases were detected. As the calcination temperature
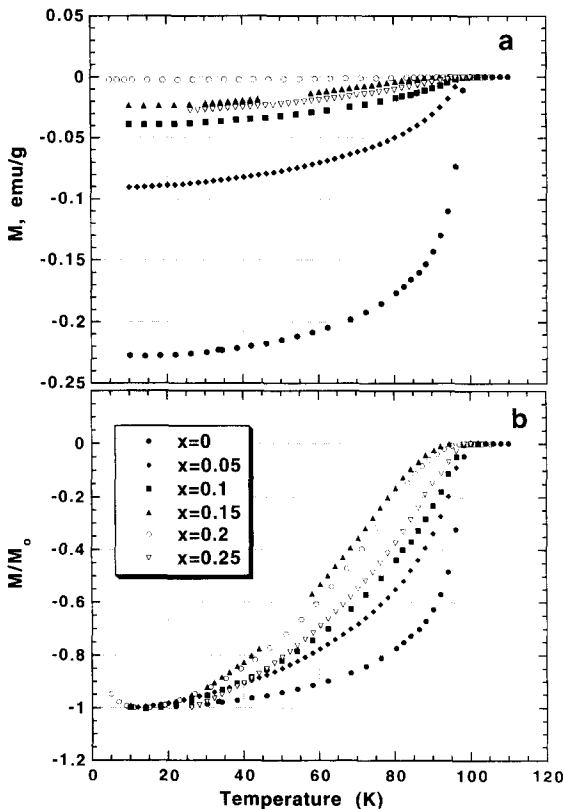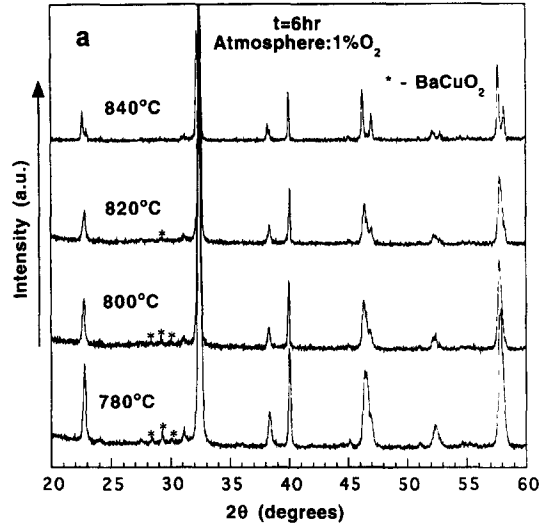

Fig. 8. Magnetization (a) and relative magnetization (b) of $Nd_{1+x}Ba_{2-x}Cu_3O_{6.5+x/2+\delta}$ powders vs. temperature, in the $0 \leq x \leq 0.25$ range.

is elevated, the orthorhombic splitting increases along with a decrease of the BaCuO$_2$ content and x. The decrease of x results also in changing the solid solution composition and its weight fraction according to reaction (3). As x decreases the atomic ratios Cu/Nd [$3/(1 + x)$] and Ba/Nd [$(2 - x)/(1 + x)$] increase up to the stoichiometric values of 3/1 and 2/1, respectively. Thus, the weight fraction of Nd123SS increases as the reaction proceeds. Since the Cu sites are assumed fully occupied infer that during the reaction some Nd ions (from Ba sites) diffuse out and some of the Ba ions penetrate into the Nd123SS cells, thus decreasing the value of x, the remaining ions build additional cells with lower x values and therefore the grains size increase (Fig. 5).

The knowledge of the exact value of x gives an important information about the progress of the reaction and the changing amount of BaCuO$_2$ in the powder during calcination. Fig. 10 illustrates the simultaneous changes in x, the BaCuO$_2$ and Nd123SS weight fractions at various calcination temperatures (after 6 hours of calcination under an atmosphere of 1% O$_2$ + 99% N$_2$). At 840°C the content of BaCuO$_2$ decreases to levels undetected by XRD analysis.

Theoretical calculations of the weight fraction of BaCuO$_2$ as a function of x for various solid solution stoichiometries are presented in Fig. 11. The solid
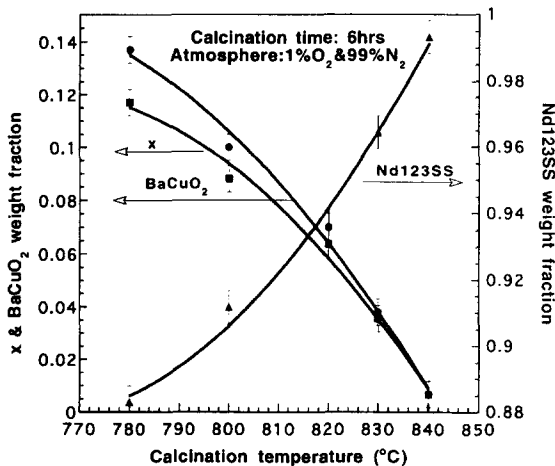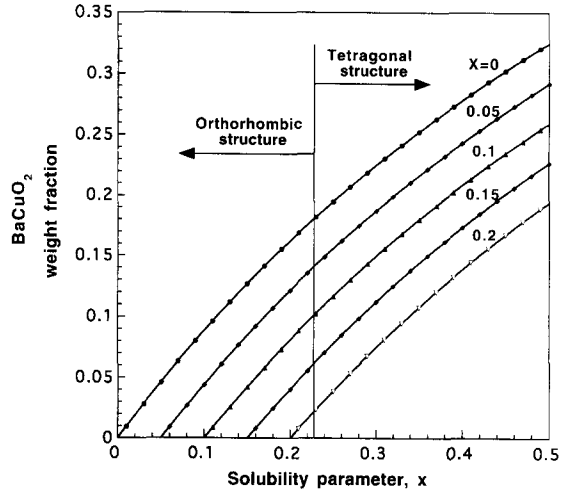

Fig. 11. Theoretical calculation of BaCuO$_2$ weight fraction in different solid solutions as a function of x, changing during its preparation.

solution reactions described by the curves in Fig. 11 for $x = 0.05$, 0.10, 0.15, 0.20 are based on the following set of equations:

$$\frac{3x - 0.15}{1 + x} BaCuO_2$$

$$+ \frac{1.05}{1 + x} Nd_{1+x}Ba_{2-x}Cu_3O_{6.5+x/2+\delta}$$

$$\rightarrow Nd_{1.05}Ba_{1.95}Cu_3O_{6.525+\delta}, \tag{4}$$

$$\frac{3x - 0.3}{1 + x} BaCuO_2$$

$$+ \frac{1.1}{1 + x} Nd_{1+x}Ba_{2-x}Cu_3O_{6.5+x/2+\delta}$$

$$\rightarrow Nd_{1.1}Ba_{1.9}Cu_3O_{6.55+\delta}, \tag{5}$$

$$\frac{3x - 0.45}{1 + x} BaCuO_2$$

$$+ \frac{1.15}{1 + x} Nd_{1+x}Ba_{2-x}Cu_3O_{6.5+x/2+\delta}$$

$$\rightarrow Nd_{1.15}Ba_{1.85}Cu_3O_{6.575+\delta}, \tag{6}$$

$$\frac{3x - 0.6}{1 + x} BaCuO_2$$

$$+ \frac{1.2}{1 + x} Nd_{1+x}Ba_{2-x}Cu_3O_{6.5+x/2+\delta}$$

$$\rightarrow Nd_{1.2}Ba_{1.8}Cu_3O_{6.6+\delta}. \tag{7}$$

Fig. 10. Effect of calcination temperature on the weight fractions of Nd123SS and BaCuO$_2$ and on the value of x during preparation of Nd123 ($x = 0$) powder.

rate of the change of x, (dx/dt), is proportional to the molar fractions of $BaCuO_2$ and Nd123SS. Based on Eq. (3) we define α and β as: $\alpha = 3x/(1 + x)$ and $\beta = 1/(1 + x)$. Using these designations we can present reaction (3) as:

$$\alpha\,BaCuO_2 + \beta\,Nd123SS \rightarrow Nd123. \qquad (8)$$
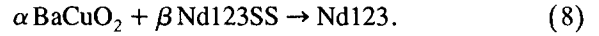
Additional assumptions concerning the solid state reaction described here are: (i) the reaction takes place in a polycrystalline homogeneous powder and the diffusion length of all ions is similar; (ii) the reaction is diffusion limited and the decreasing contact area between the particles may be represented by the coefficients α and β.

As the Nd123SS and $BaCuO_2$ react, α decreases and β increases. Based on the assumptions above, the reaction rate is expected to be of the following form:

$$\frac{\partial\alpha}{\partial t} = -K(T)\alpha\beta = \frac{\partial\alpha}{\partial x}\frac{\partial x}{\partial t}$$

$$\frac{\partial\beta}{\partial t} = +\frac{1}{3}K(T)\alpha\beta = \frac{\partial\beta}{\partial x}\frac{\partial x}{\partial t}, \qquad (9)$$

where K is the reaction rate coefficient and depends on the calcination temperature only. From the definitions of a and b, it is clear that the disappearance rate of $BaCuO_2$ is three times larger than the forma-
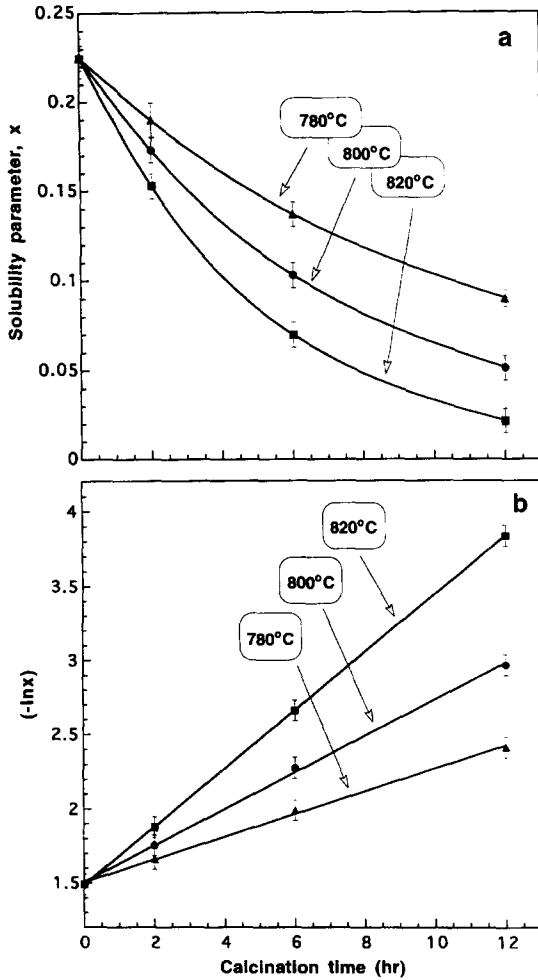
Fig. 12. (a) Effect of Nd123 powder calcination time on x during the calcination of Nd123 powder and (b) a linear fit of Eq. (11) at different temperatures.

For any solid solution stoichiometry, x can be evaluated from XRD data. Using x and the target stoichiometry, Fig. 11 enables an exact evaluation of $BaCuO_2$ weight fraction left in the system independent of the calcination conditions. Fig. 12a shows the effect of calcination time, t, on x at different calcination temperatures. The value of x decreases as the reaction proceeds and as expected, at higher temperatures it decreases faster. The solid lines are cubic spline fits to the experimental data.

We suggest a kinetic model for the description of Nd123 formation based on the assumption that the
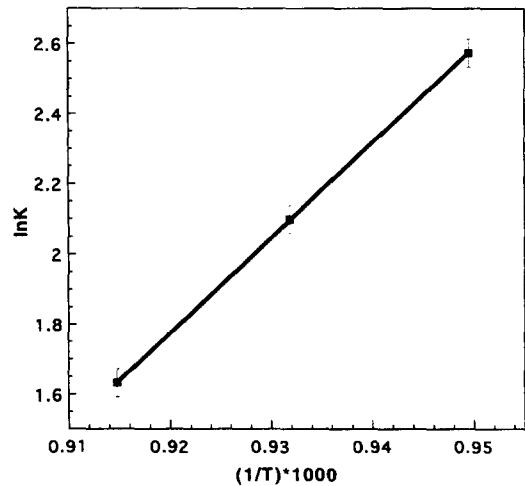

Fig. 13. Variation of the reaction rate constant, K, with calcination temperature.
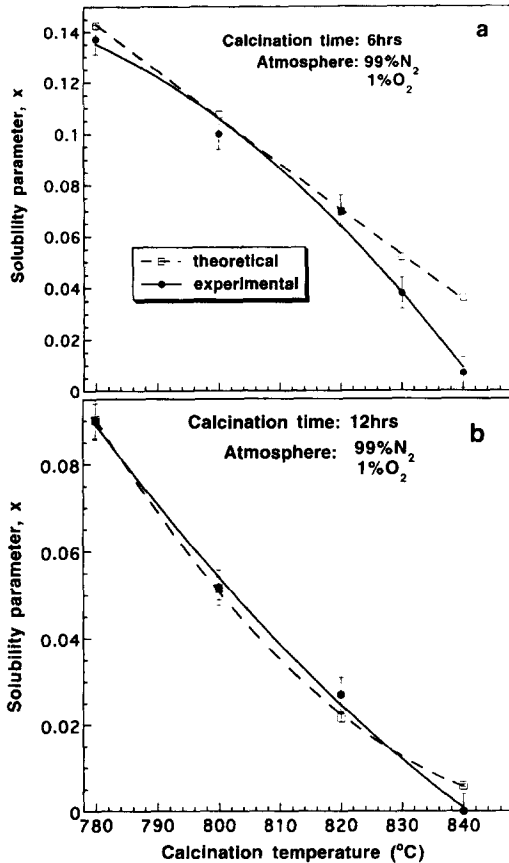
Fig. 14. Effect of calcination temperature on x at (a) 6 hours and (b) 12 hours: comparison of calculated and experimental results.

tion rate of Nd123SS. Differentiation of α and β by x and substitution into Eq. (9) yields:

$$\frac{\partial x}{\partial t} = -Kx. \tag{10}$$

The initial condition is: $x = x_0$ at $t = 0$ was obtained experimentally. Integration of Eq. (10) yields:

$$x = x_0 \exp(-Kt) \quad \text{or} \quad -\ln x = -\ln x_0 + Kt, \tag{11}$$

which is plotted in Fig. 12b (solid lines) at different temperatures. All lines have a common intercept at $x_0 = 0.225 \pm 0.007$, which is very close to the orthorhombic–tetragonal phase transformation point. This is the minimal value of x after the vacuum

stage, showing that the initial solid solution is favored in the tetragonal form. The value of x was also determined experimentally as shown in Fig. 12b to assure the consistency of Fig. 12b and investigate it in a wide range of orthorhombicity. The slope of the lines in Fig. 12b represents the reaction rate constant, K. The diffusion coefficient of the reaction is given by: $D = D_0 \exp(-E_a/RT)$. The temperature dependence of K also follows the Arrhenius equation, $K = K_0 \exp[-E_a/RT]$ as expected from its major dependence on diffusion coefficient ($K \sim D$). E_a is the effective activation energy for the diffusion limited reaction (8) and K_0 is the pre-exponential constant which is assumed to be weakly dependent on the temperature. A linear regression between ln K and $1/T$ proving that the reaction rate constant follows the Arrhenius equation is shown in Fig. 13. The slope and the intercept of the regression are $E_a = 54.2$ Kcal/mol (2.35 eV), and $K_0 = 1.13 \times 10^{10}$ hr^{-1}, respectively. The effective activation energy for the occurrence of reaction (8) in the way suggested, is of the same order of magnitude as activation energies obtained for oxygen in-diffusion for YBCO [20,23–28]. Since K increases with the temperature, the reaction is expected to be endothermic. Fig. 14 demonstrates the effect of the calcination temperature on the value of x after 6 and 12 hours of calcination. Combining the Arrhenius equation of the rate constant with Eq. (11), the temperature dependence of x is given by:

$$x = x_0 \exp[-K_0 \exp(-E_a/RT)t]. \tag{12}$$

Substituting numerical values of x_0, E_a, K_0 and t (6 or 12 hours) we get an expression which depends only on the calcination temperature. Fig. 14 also illustrates the comparison between the experimental and the model derived values of x after 6 and 12 hours. As can be seen there is a significant deviation between the experimental and the modeled values of x above 820°C. We attribute the deviation to the formation of liquid phase whose evidence is seen in Fig. 5 as discussed earlier. The occurrence of a liquid phase at high temperatures (> 820°C), allows the reaction to occur faster and reduces the value of x quicker than the model suggests. The agreement between the model and the experimental data is improved at longer calcination times.

4. Conclusions

The formation and properties of the solid solutions $Nd_{1+x}Ba_{2-x}Cu_3O_{6.5+x/2+\delta}$ (Nd123SS) in the wide compositional range of $0 \leq x \leq 0.25$ has been investigated. Various ways to identify the $BaCuO_2$ content and the value of x in the solid solution system were evaluated. The methods include: (i) evaluating the unit cell parameters; (ii) calculating the orthorhombic splitting (OS) factor; (iii) calibrating the distance between the (020) and (200) reflections; (iv) evaluating the melting point temperature. The method based on calculation of the OS factor from XRD data is most accurate, yet method (iii) is the fastest. A general scheme to determine the value of x from XRD data was developed by knowing the target stoichiometry and the unit cell parameters.

It has been found that the formation of Nd123 ($x = 0$) superconducting powder goes through the reaction between $BaCuO_2$ and the Nd123SS. A kinetic model, using x as the kinetic parameter, was developed to describe the reaction as a function of calcination time and temperature. The model fits the data well below 820°C. However, above this temperature for $x < 0.05$, a liquid phase is present accelerating diffusion, thus increasing the rate of the reaction and decreasing the value of x faster than the model predicts. The effective activation energy of the solid state reaction was found to be 54.2 Kcal/mol (2.35 eV). This effective activation energy is of the same order of magnitude as that of the oxygen diffusion in the Y123 superconducting system. The correlation between the SA, particle size, morphology and x is consistent with the diffusion limited solid state reaction of $BaCuO_2$ and Nd123SS. Finally, high values of T_c (measured by DC magnetization) were found in the powders. The highest T_c of 98.7 K was obtained for the $x = 0$ case. This value is the highest ever reported in the Nd–Ba–Cu–O system. The T_c was found to be insensitive to the value of x, ranging between 98.7 and 94 K for x between 0 and 0.25, respectively.

Acknowledgements

References

[1] S.I. Yoo, M. Murakami, N. Sakai, T. Higuchi and S. Tanaka, Jpn. J. Appl. Phys. 33 (1994) L998.

[2] D.N. Matthews, J.W. Cochrane and G.J. Russel, Physica C 249 (1995) 255.

[3] A. Takagi, T. Yamazaki, T. Oka, Y. Yanagi, Y. Itoh, M. Yoshikawa, Y. Yamada and U. Mizutani, Physica C 250 (1995) 222.

[4] M. Murakami, S.I. Yoo, T. Higuchi, N. Sakai, J. Weltz, N. Koshizuka and S. Tanaka, Jpn. J. Appl. Phys. 33 (1994) L715.

[5] W. Bieger, G. Krabbes, P. Schätzle, L. Zelenina, U. Wiesner, P. Verges and J. Klosowski, Physica C 257 (1996) 46.

[6] A.A. El-Hamalaway, I. Halasz, M.T. Daoud, E.A. Ghali and M.A. El-Zaidia, Phys. Status Solidi 140 (1993) 213.

[7] W. Wong-Ng, B. Paretzkin and E.R. Fuller, J. Solid State Chem. 85 (1990) 117.

[8] K. Zhang, B. Dabrowski, C.U. Segre, D.G. Hinks, I.K. Schuller, J.D. Jorgensen and M. Slaski, J. Phys. C: Solid State Phys. 20 (1987) L935.

[9] S.I. Yoo and R.W. McCallum, Physica C 210 (1993) 147.

[10] F. Sujia, X. Shisheng, L. Jingkui, C. Guaungchang and Z. Zongxiang, Mod. Phys. Lett. B 2 (1988) 1073.

[11] H. Nozaki, S. Takekawa and Y. Ishizawa, Jpn. J. Appl. Phys. 27 (1988) L31.

[12] M.J. Kramer, A. Karion, K.W. Dennis, M. Park and R.W. McCallum, J. Electron. Mater. 23 (1994) 1117.

[13] F. Izumi, S. Takekawa, Y. Matsui, N. Iyi, H. Asano, T. Ishigaki and N. Watanabe, Jpn. J. Appl. Phys. 26 (1987) L1616.

[14] K. Takita, H. Akinaga, H. Katoh and K. Masuda, Jpn. J. Appl. Phys. 27 (1988) L1676.

[15] M.J. Kramer, S.I. Yoo, R.W. McCallum, W.B. Yelon, H. Xie and P. Allenspach, Physica C 219 (1994) 145.

[16] K. Takita, H. Akinaga, H. Katoh and K. Masuda, Jpn. J. Appl. Phys. 27 (1988) L607.

[17] T. Itoh, M. Uzawa and H. Uchikawa, J. Am. Ceram. Soc. 7 (1988) C188.

[18] G.E. Shter and G.S. Grader, J. Am. Ceram. Soc. 77 (1994) 1436.

[19] P. Yossefov, G.E. Shter, G.M. Reisner and G.S. Grader, in preparation, 1996.

[20] K.N. Tu, N.C. Yen, S.I. Park and C.C. Tsuei, Phys. Rev. B 39 (1989) 304.

[21] K. Takita, H. Akinaga, H. Katoh, H. Asano and K. Masuda, Jpn. J. Appl. Phys. 27 (1988) L67.

[22] K. Takita, H. Katoh, H. Akinaga, M. Nishino, T. Ishigaki and H. Asano, Jpn. J. Appl. Phys. 27 (1988) L57.

[23] K.N. Tu and L.T. Shi, Appl. Phys. Lett. 55 (1989) 1351.

[24] S.J. Rothman, J.L. Routbort and J.E. Baker, Phys. Rev. B 40 (1989) 8852.

[25] M.V. Patrakeev, I.A. Leonidov, V.L. Kozhevnikov, V.I. Tsidilkovaskii, A.K. Demin and A.V. Nikolaev, Solid State Ionics 66 (1993) 61.

[26] S.J. Rothman, J.L. Routbort, U. Welp and J.E. Baker, Phys. Rev. B 44 (1991) 2326.

[27] E. Salomons and D. De-Fontaine, Phys. Rev. B 41 (1990) 11159.

[28] M.S. Islam and R.C. Baetzold, J. Mater. Chem. 4 (1994) 299.

[29] D.V. Fomichev, O.G. D'yachenko, A.V. Mironov and E.V. Antipov, Physica C 225 (1994) 25.

[30] G.D. Chryssikos, E.I. Kamitsos, J.A. Kapoutsis, A.P. Patsis, V. Psycharis, A. Koufoudakis, Ch. Mitros, G. Kallias, E. Gamari-Seale and D. Niarchos, Physica C 254 (1995) 44.